WEHI
brighter together

The Walter and Eliza Hall Institute of Medical Research
ABN 12 004 251 423
1G Royal Parade Parkville Victoria 3052 Australia
T +61 3 9345 2555 F +61 3 9347 0852
www.wehi.edu.au

Research Publication Repository
http://publications.wehi.edu.au/search/SearchPublications

This is the peer reviewed version of the following article, which has been published in final form at the link below.

Publication details:	Ishihara K, Shimizu R, Takata K, Kawashita E, Amano K, Shimohata A, Low D, Nabe T, Sago H, Alexander WS, Ginhoux F, Yamakawa K, Akiba S. Perturbation of the immune cells and prenatal neurogenesis by the triplication of the Erg gene in mouse models of Down syndrome. *Brain Pathology.* 2020 30(1):75-9
Published version Is available at:	https://doi.org/10.1111/bpa.12758

Changes introduced as a result of publishing processes such as copy-editing and formatting may not be reflected in this manuscript.

This article may be used for non-commercial purposes in accordance with Wiley Terms and Conditions for Use of Self-Archived Versions. This article may not be enhanced, enriched or otherwise transformed into a derivative work, without express permission from Wiley or by statutory rights under applicable legislation. Copyright notices must not be removed, obscured or modified. The article must be linked to Wiley's version of record on Wiley Online Library and any embedding, framing or otherwise making available the article or pages thereof by third parties from platforms, services and websites other than Wiley Online Library must be prohibited.

DR KEIICHI ISHIHARA (Orcid ID : 0000-0001-8748-7218)

Article type : Research Article

Perturbation of the immune cells and prenatal neurogenesis by the triplication of the *Erg* gene in mouse models of Down syndrome

Keiichi Ishihara[1]*¶, Ryohei Shimizu[1¶], Kazuyuki Takata[2,3,4], Eri Kawashita[1], Kenji Amano[5], Atsushi Shimohata[5], Donovan Low[4], Takeshi Nabe[6], Haruhiko Sago[7], Warren S. Alexander[8,9], Florent Ginhoux[4,10], Kazuhiro Yamakawa[5], and Satoshi Akiba[1]

[1] Department of Pathological Biochemistry, Division of Pathological Sciences, [2] Department of Clinical and Translational Physiology, Division of Biological Sciences, [3]Division of Integrated Pharmaceutical Sciences, Kyoto Pharmaceutical University, Kyoto 607-8414, Japan

This article has been accepted for publication and undergone full peer review but has not been through the copyediting, typesetting, pagination and proofreading process, which may lead to differences between this version and the Version of Record. Please cite this article as doi: 10.1111/bpa.12758

This article is protected by copyright. All rights reserved.

Accepted Article

[4] Singapore Immunology Network (SIgN), Agency for Science, Technology and Research (A*STAR), 8A Biomedical Grove, IMMUNOS Building #3-4, BIOPOLIS, 138648, Singapore

[5] Laboratory for Neurogenetics, RIKEN Center for Brain Science, Saitama 351-0198, Japan

[6] Laboratory of Immunopharmacology, Faculty of Pharmaceutical Sciences, Setsunan University, Osaka, Japan

[7] Center for Maternal-Fetal, Neonatal and Reproductive Medicine, National Center for Child Health and Development, Tokyo, Japan

[8] Cancer and Haematology Division, The Walter and Eliza Hall Institute of Medical Research, Parkville, Australia

[9] Department of Medical Biology; University of Melbourne; Parkville, Australia

[10] Shanghai Institute of Immunology, Shanghai Jiao Tong University School of Medicine, 280 South Chongqing Road, Shanghai 200025, China

¶ These authors also contributed equally to this work.

This article is protected by copyright. All rights reserved.

Accepted Article

Accepted Article

*To whom correspondence should be addressed: Keiichi Ishihara, Ph.D.

Lecturer, Department of Pathological Biochemistry, Kyoto Pharmaceutical University, 5 Misasagi Nakauchi-cho, Yamashina-ku, Kyoto 607-8414, Japan. Tel: +81-75-595-4656; Fax: +81-75-595-4759; E-mail: ishihara@mb.kyoto-phu.ac.jp

Running title: Triplication of the *Erg* in DS brain

Keywords: Down syndrome, mouse models, immune cells, transcriptomics, transcriptional factor Erg, prenatal neurogenesis

Abstract

Some mouse models of Down syndrome (DS), including Ts1Cje mice, exhibit impaired prenatal neurogenesis with yet unknown molecular mechanism. To gain insights into the impaired neurogenesis, a transcriptomic and flow cytometry analysis of E14.5 Ts1Cje embryo brain was performed. Our analysis revealed that the neutrophil and monocyte ratios in the CD45-positive

This article is protected by copyright. All rights reserved.

Accepted Article

hematopoietic cells were relatively increased, in agreement with the altered expression of inflammation/immune-related genes, in Ts1Cje embryonic brain, whereas the relative number of brain macrophages was decreased in comparison to wild-type mice. Similar upregulation of inflammation-associated mRNAs was observed in other DS mouse models, with variable trisomic region lengths. We used genetic manipulation to assess the contribution of *Erg*, a trisomic gene in these DS models, known to regulation hemato-immune cells. The perturbed proportions of immune cells in Ts1Cje mouse brain were restored in Ts1Cje-Erg$^{+/+/Mld2}$ mice, which are disomic for functional Erg but otherwise trisomic on a Ts1Cje background. Moreover, the embryonic neurogenesis defects observed in Ts1Cje cortex were reduced in Ts1Cje-Erg$^{+/+/Mld2}$ embryos. Our findings suggest that *Erg* gene triplication contributes to the dysregulation of the homeostatic proportion of the populations of immune cells in the embryonic brain and decreased prenatal cortical neurogenesis in the prenatal brain with DS.

INTRODUCTION

Down syndrome (DS), which is caused by an additional copy of chromosome 21 (HSA21), is the most common aneuploidy and genetic cause of intellectual disability (30, 14). Various symptoms,

This article is protected by copyright. All rights reserved.

Accepted Article

including learning disabilities, distinctive craniofacial phenotypes and hypotonia are exhibited in most individuals with DS (14). The results of post-mortem analyses of brain specimens suggest that retardation of prenatal neurogenesis and postnatal degeneration of the cortical pyramidal neurons occurs in the brains of individuals with DS (42). It can therefore be hypothesized that the neurological deficits in prenatal life could be closely involved in the intellectual disability of individuals with DS, and the identification of the gene(s) dysregulated in HSA21 that contribute to the neurological abnormalities of individuals with DS, such as impaired neurogenesis and neuronal degeneration, is an important goal of DS research.

Several mouse models of DS can be used to investigate the etiology of DS (see reviews in 20, 40, 56). The distal end of mouse chromosome 16 (MMU16) shows conserved synteny with a large portion of human HSA21. Mice carrying an extra segment of MMU16, such as Ts(17^{16})65Dn (hereafter called Ts65Dn) (7), Ts[Rb(12.17^{16})]2Cje (50), Ts(12^{16}C-tel)1Cje (Ts1Cje) (41) and Dp(16Cbr1-Fam3b)1Rhr/J (Ts1Rhr) (35), are therefore widely used as animal models of DS. Ts65Dn mice carrying approximately 90 triplicated genes as an extra chromosome exhibit pathological features that are close to those of humans with DS, including learning and memory impairment (39) and impaired prenatal neurogenesis (6). Additionally, Ts2Cje mice were established after a fortuitous translocation of the Ts65Dn marker chromosome to MMU12 (50). Ts1Cje mice carry a shorter

This article is protected by copyright. All rights reserved.

trisomic segment (with approximately 70 genes) in comparison to Ts65Dn/Ts2Cje mice and exhibit milder cognitive impairment than Ts65Dn mice (41). Ts1Cje and Ts2Cje mice exhibit similar degrees of prenatal cortical neurogenesis impairment and adult neurogenesis impairment (25). In addition, Ts1Rhr mice carry a trisomic region of approximately 30 orthologs that is shorter than that in Ts1Cje mice (35) and exhibit some of the abnormal phenotypes observed in Ts65Dn and Ts1Cje mice, including decreased long-term potentiation (LTP) in the fascia dentate, enlargement of the dendritic spines and a decreased spine in fascia dentate, disturbed working memory, as assessed by T-maze test (3), and enlarged brain ventricles (38). Altogether, these observations suggest that the gene(s) responsible for neurogenesis impairment might be located on the Ts1Cje trisomic region. However, the detailed molecular mechanisms underlying the abnormal phenotypes observed in mouse models of DS remain unknown.

Characterization of gene expression in the DS brain, including animal models, is helpful for understanding the molecular mechanism underlying DS phenotypes. Indeed, several comparative gene expression-profiling studies have been carried out in fetal brains, amniocytes, neurospheres, and cell lines derived from individuals with DS (see review in 24). Unraveling parallelly the molecular perturbation in the brain of DS mouse models at the prenatal neurogenic stage is expected to help understanding the molecular mechanisms underlying the impaired cortical neurogenesis in DS. In the

This article is protected by copyright. All rights reserved.

Accepted Article

present study, a comparative transcriptomics analysis of the Ts1Cje embryo brain revealed the increased expression of molecules enriched in inflammatory cells, such as neutrophils and monocytes. The fetal brain also showed abnormalities in the ratios and morphology of brain macrophages. Using an *in vivo* gene-subtraction strategy, we also demonstrated that the disturbed distribution of immune cells, such as neutrophils, monocytes and brain macrophages, and the impaired prenatal neurogenesis in Ts1Cje embryos were caused, at least in part, by the triplication of *Erg* gene, which is located in the trisomic region.

MATERIALS AND METHODS

Mice – Ts1Cje and Dp(16Cbr1-ORF9)1Rhr (Ts1Rhr, from Jackson Lab. Stock 005383) mice were maintained by crossing carrier males with C57BL/6J females (N30 and N6, respectively). Genotyping of Ts1Cje and Ts1Rhr mice was performed by polymerase chain reaction (PCR) as previously described (41, 35). Mouse embryos were derived from crossing Ts1Cje or Ts1Rhr males and C57BL/6J females and the day of vaginal plug was considered to be E0.5. Ts[Rb(12.17^{16})]2Cje (Ts2Cje) (50) mice were maintained by crossing carrier females with (C57BL/6JEiJ × C3Sn.BLiA-$Pde6b^{+}$/DnJ)F1/J males. Genotyping of Ts2Cje mice was performed by a PCR using multiplex

This article is protected by copyright. All rights reserved.

Accepted Article

primers as previously described (12). Mouse embryos were derived from crossing of Ts2Cje females and (C57BL/6JEiJ × C3Sn.BLiA-Pde6b^{+}/DnJ)F1/J males. To generate Ets2$^{+/-}$ mice, the *Ets2* gene was targeted by homologous recombination in 129-ES cells with a targeting vector designed to replace all or part of three exons, exon 8-10 of the gene coding for the Ets binding domain with the neomycin cassette (57) (Supplementary Figure S1). Ets2$^{+/-}$ mice that were backcrossed at least 17 generations with C57BL/6J mice were used. Erg$^{+/Mld2}$ mice were generated on a C57BL/6J background by N-ethyl-N-nitrosourea (ENU) mutagenesis and then maintained by mating heterozygous Erg$^{+/Mld2}$ mice with C57BL/6J mice (33). ENU mutagenesis induced a thymidine to cystosine transition that resulted in an amino acid substitution of proline for serine at position 329 (S329P). This amino acid substitution reduces the transactivation activity of the protein. Fewer than five mice were housed per cage on a 12-h light–dark cycle. The mice had *ad libitum* access to food and water. All experimental procedures were performed in accordance with the guidelines of the Animal Experiments Committee of Kyoto Pharmaceutical University and the RIKEN Brain Science Institute.

Microarray – Total RNA of the embryonic brain was extracted using RNAiso (Takara Bio, Shiga, Japan) according to the manufacturer's instructions, followed by treatment with DNase I. The Low Input Quick Amp Labeling kit (Agilent Technologies, Santa Clara, CA, USA) was used to synthesize

This article is protected by copyright. All rights reserved.

Accepted Article

Cy3-labeled cRNA probes from 100 ng of total RNA. Hybridization was carried out on a SurePrint G3 Mouse GE microarray kit 8×60K (Agilent Technologies) and the array was scanned with an Agilent G2565CA Microarray Scanner System (Agilent Technologies). The fluorescence intensity on scanned images was quantified, and the values were corrected for the background level and normalized with the Feature Extraction software program (version A.8.5.1; Agilent Technologies). The raw microarray data from three male embryos in each genotype were further analyzed. For the identification of the differential expression between WT and Ts1Cje mice, the genes were required to pass two criteria: a ratio beyond the 99.5% confidence interval observed in homotypic comparisons, which corresponded to a ~1.5-fold expression change and statistical significance ($p < 0.05$) in a paired t-test (31). Correction for multiple comparisons was performed using the adjusted Benjamini-Hochberg FDR (http://www.chem-agilent.com/cimg/mtc.pdf). We have deposited the raw, unfiltered data (accession no. GSE121449) to the public repository, Gene Expression Omnibus (GEO) at NCBI (http://www.ncbi.nlm.nih.gov/geo/).

Bioinformatics analyses – The functional annotation analysis of RNA transcripts with differential expression in the brains of Ts1Cje mice was performed using the Database for Annotation, Visualization, and Integrated Discovery (DAVID) version 6.7 (http://david.abcc.ncifcrf.gov/home.jsp)

This article is protected by copyright. All rights reserved.

(10, 22). A 'gene list' of all target genes (all genes in Supplementary Tables S1 and S2) except for genes with no GI ID that were differentially expressed in Ts1Cje mice in comparison to WT mice was compiled and uploaded to the DAVID web interface using the MGI ID against the whole mouse genome (Supplementary Table S3).

Quantitative RT-PCR– Total RNA (5 μg) treated with DNase I was reverse-transcribed using random hexamers and ReverTra Ace reverse transcriptase (Toyobo Co., Osaka, Japan). The qRT-PCR cDNA samples were analyzed using SYBR-Green I (Takara Bio) and a LightCycler® Nano system (Roche Applied Science, Mannheim, Germany). The primers and PCR conditions are shown in Supplementary Table S4. The relative standard curve method was used to analyze the gene expression. After parallel amplification, the expression levels were normalized to the expression of 18S ribosomal RNA.

Western blotting – Proteins were extracted from the brains of WT and Ts1Cje embryos (E14.5). Protein extracts (25 μg) were subjected to SDS-15% PAGE, and blotted onto nitrocellulose membranes. The membranes were incubated with S100 calcium-binding protein A9 (S100A9)

This article is protected by copyright. All rights reserved.

(1:2000, AF2065, Research & Diagnostic Systems, Minneapolis, MN, USA) and β-actin (1:5000 dilution, A5441, Sigma-Aldrich, St. Louis, MO, USA) antibodies. The membranes were exposed to anti-goat or anti-mouse secondary antibody conjugated with horseradish peroxidase (1:10,000), and then bands were detected by using a Chemi-lumi One Super (Nacalai Tesque, Kyoto, Japan) with the LAS-3000 mini image analysis system (Fujifilm, Tokyo, Japan). The intensity of band was quantified using the NIH Image J software program (developed at U.S. National Institutes of Health and available on the Internet at http://rsb.info.nih.gov/nih-image/) using a gel analysis macro.

Flow cytometry– The fetal brain was removed, washed with PBS containing 2mM EDTA and settled in a 48-well plate. The brains were transferred into new wells filled with 0.2 mg/mL collagenase (type IV, Sigma-Aldrich) in RPMI medium containing 10% fetal calf serum (FCS), minced, and incubated for 30 min at 37°C, and single-cell suspensions were generated by filtration through a sterile 70-μm cell strainer (BD Biosciences, San Jose, CA, USA). After washing with a buffer (0.5% [w/v] BSA, 2 mM EDTA in PBS), cells were stained with antibodies (Supplementary Table S5) in blocking buffer containing mouse and rat serum. 7-aminoactinomycin D (7-AAD) was used to remove dead cells. All flow cytometry analyses were run using an LSRFortessa flow cytometer (BD Biosciences) and analyzed using the Kaluza software program (Beckman Coulter, Brea, CA, USA).

This article is protected by copyright. All rights reserved.

Accepted Article

Immunohistochemistry and image analyses – Brain sections were incubated with biotin-conjugated rat anti-mouse F4/80 (AbD Serotec, Raleigh, NC, USA, MCA497B, 1:200 in PBST) overnight at 4°C after treatment with 3% H_2O_2 in PBST (PBS containing 0.3% Triton X-100) for 15 min at room temperature, after avidin and biotin blocking (each 15 min at room temperature) (Vector Labs, Burlingame, CA, USA) and blocking with blocking solution (0.2% bovine serum albumin in PBST). Immunoreactivity for F4/80 was amplified with a TSA Biotin System (Perkin Elmer, Waltham, MA, USA) according to the manufacturer's instruction, after incubation with streptavidin HRP (1:100; PerkinElmer) for 30 min, and the sections were then incubated with streptoavidin-Cy3 (1:500, Thermo Fisher Scientific, Waltham, MA, USA) for 2 hours. Photomicrographs were acquired using a confocal laser microscope Zeiss LSM800 (Carl Zeiss, Oberkochen, Germany). The density of cells (cells/mm^2) stained with anti-F4/80 antibody was measured by an image analysis using coronal sections of E14.5 mice (n = 3 in each genotype). In brief, the immunofluorescent images of fetal brain sections were obtained on a laser confocal microscope (LSM800). The entire fetal brain region inside the meninges was outlined in each brain section. The area of the outlined regions and the number of F4/80-immunoreactive cells were analyzed using the ImageJ software program. The density of F4/80-immunoreactive cells in the brain was calculated using the obtained values. As indicators of cell

This article is protected by copyright. All rights reserved.

morphology, cell circularity was analyzed using the Image J software program (public domain Java image processing program) with the BioFormat plugin, as described previously (58).

In vivo BrdU labeling – BrdU (50 mg/kg body weight) was administered to a pregnant female (E13.5). At twenty-four hours after the injection, frozen brain sections (50-µm thickness) were prepared, and stained with antibodies against Ki67 (1:500; Novacastra, Norwell, MA, USA) and BrdU (1:200; BD Biosciences, Franklin Lakes, NJ) after 2M HCl-treatment (30 min at room temperature), neutralization with 0.1 M boric acid pH 8.5 (10 min at room temperature), Mouse on Mouse blocking (Vector Laboratories), and a blocking process with blocking solution (0.3% Triton X-100 and 4% Blockace (DS Pharma Co. Osaka, Japan) in PBS). The embryonic brain sections were then incubated for 1 hour at room temperature with Alexia 594-conjugated donkey anti-rabbit IgG (1:400; Invitrogen, Carlsbad, CA, USA) and Alexia 488-conjugated donkey anti-mouse IgG (1:400; Invitrogen). Nuclei were then stained with 4',6-diamino-2-phenylindole (DAPI), and coverslipped in Prolong Gold™ antifade reagent (Invitrogen). Photomicrographs were acquired using a confocal laser microscope NIKON A1R (Nikon). BrdU(+)/Ki67(-) cells were counted in each slice by three-dimensional counting under a confocal microscope (acquired 25 µm-thick z-stack images [1 µm steps]). The numbers of $BrdU^+$ $Ki67^-$ cells and nuclei stained with DAPI were counted according to three-

This article is protected by copyright. All rights reserved.

dimensional cell-counting methods (counting box: 150 × 180 × 25 µm) (54). Counting was performed in 16-20 cerebral cortices of each genotype [n = 10 (WT), 9 (Ts1Cje), and 8 (Ts1Cje-Erg$^{+/+/Mld2}$)] in a blinded manner.

The numbers of BrdU^{+} Ki67^{-}cells in WT, Ts1Cje, and Ts1Cje-Erg$^{+/+/Mld2}$ mice (n = 3 in each genotype) were recorded according to the following stereological methods: Seven sections (every third section, 50 µm thickness) were immunostained with antibodies for BrdU and Ki67. Confocal images were then acquired using a confocal laser microscope NIKON A1R (acquired 50 µm-thick z-stack images [1 µm steps]) and uploaded to the StereoInvestigator software program (MBF Bioscience, Williston, VT, USA). The stereological parameters were as follow: sampling grid 63.2 µm × 63.2 µm, counting frame 20 µm × 20 µm, guard zone 5 µm, dissector height 10 µm. The values for the coefficient of error (CE; Gundersen m = 1), which was considered appropriate when below 0.10, ranged from 0.05-0.07.

Statistical analyses – Data are indicated as the mean ± standard error of means (SEM). Differences between two genotypes were analyzed using the Student's t test, whereas multiple genotype

This article is protected by copyright. All rights reserved.

comparisons were performed using a one-way analysis of variance (ANOVA) followed by an LSD post-hoc test. $p < 0.05$ was considered as the lowest level of significance.

RESULTS

Transcriptomic profiling in the brain of Ts1Cje mouse embryos

Whole mouse genome microarrays (probes for 39,430 gene products and 16,251 lincRNAs) were employed to identify the molecules involved in the developmental delay of Ts1Cje brains. Gene expression profiles were evaluated on embryonic day (E) 14.5, when decreased neocortical neurogenesis is observed in Ts1Cje embryos (25). The expression levels of 61 transcripts, including 21 genes coded within the trisomic region, were found to differ significantly between wild-type (WT) and Ts1Cje mice (>1.5-fold change, $p<0.05$) (Supplementary Tables S1 and S2). To confirm the gene-dosage dependent overexpression of the triplicated genes in the brain of Ts1Cje embryos, the expression data of the triplicated genes were extracted and summarized (Figure 1). Although fewer than one-third of the triplicated genes in Ts1Cje mice showed a significantly increased expression of approximately 1.5-fold, a number of genes showed a tendency toward an increased expression. Not all genes coded on the trisomic region, however, showed upregulated expression; some mRNAs, Marp,

This article is protected by copyright. All rights reserved.

Accepted Article

Kcne1, Kcnj6, Kcnj15, Itgb2l, Fam3b, Mx1, and Tmprss2 were absent in the brain of mice at E14.5. Additionally, the levels of Scaf4, Olig2 and Cldn14 mRNA in Ts1Cje embryos were comparable to those in WT mice. In contrast, the 33 disomic genes and three genes on the chromosome X were dysregulated in E14.5 Ts1Cje brain (Supplementary Tables S1 and S2). To validate these results, we performed real-time quantitative reverse transcription PCR (qRT-PCR) analysis using the individual samples from the microarray analysis to analyze some of the differentially expressed genes. The magnitude of changes in the expression of Stfa1, Stfa2, Stfa3, Ly6c1, S100a8 and S100a9 mRNAs in Ts1Cje embryo brain were similar to the alterations demonstrated by the microarray analysis (Figure 2A). While antibodies against Stfa1, Stfa2, Stfa3 and Ly6c1 proteins for Western blotting were not commercially available, we did validate the upregulation of S100a9, which is known as an inflammation marker (49), at the protein level by Western blotting (Figure 2B, C), with approximately 8-fold higher protein expression in Ts1Cje mice than WT mice. A functional annotation analysis using the DAVID Functional Annotation tool (10, 22) was performed on 59 genes with expression that showed a 1.5-fold increase or decrease (Supplementary Table S3). The enriched functional annotation terms were “antimicrobial”, “thiol protease inhibitor”, “calcium”, “bacteriolytic enzyme”, “secreted”, “disulfide bond”, “protease inhibitor”, “antioxidant”, “signal”, “inflammatory response”, “endosome”, and “cell adhesion” (Supplementary Table S6).

This article is protected by copyright. All rights reserved.

Accepted Article

Accepted Article

Inflammation/immunity-related genes are upregulated in multiple mouse models of DS

It has been shown that the translocation of MMU16 to MMU12 introduces a monosomy of seven genes in the most telomeric part of MMU12 (~2 Mb) in Ts1Cje mice (12) (Supplementary Figure S2A). The MMU12 translocation breakpoint is located in exon 35-41 of the *Dnahc11* gene, and the expression of truncated mRNA for Dnahc11 has been shown to increase in the brain of Ts1Cje mice at 8-10 weeks of age (19). As expected, we also detected the increased expression of Dnahc11 mRNA and decreased expression of Itgb8 mRNA in Ts1Cje mice but not in other mouse models without a monosomic region (Supplementary Figure S2B, C). Since it would be better to use other mouse models of DS to confirm the changes in the expression of mRNAs that are altered in Ts1Cje mice, we next examined the expression of S100a8, S100a9, Ly6c1, Stfa1, Stfa2 and Stfa3 mRNAs in two additional models, Ts2Cje (50) and Ts1Rhr mice (35), which carry 3 copies of ~90 and ~30 MMU16 genes, respectively (Figure 3A). In both mouse models, the expression levels of all the examined genes were significantly increased in comparison to control WT mice (Figure 3B). However, the expression of Ly6c1 and Stfa2 mRNA was significantly different between Ts2Cje and Ts1Rhr mice (Figure 3B), possibly due to the existence of a specific modifier in the Ts2Cje trisomic region that is absent in Ts1Rhr mice or differences in the genetic background between the two lines. To avoid the effects of the genetic background, we tried to cross the Ts2Cje mice on a B6/C3H hybrid background

This article is protected by copyright. All rights reserved.

with C57BL/6J mice. Unfortunately, we failed to obtain any pups (beyond the sixth generation). Taken together, our results demonstrate that the increased expression of inflammation/immunity-related genes in the embryonic brain is a common abnormal phenotype in DS mouse models.

Triplication of the Erg gene causes the increased expression of disomic inflammation/immunity-related genes in the Ts1Cje embryonic brain

We found that the expression levels of some inflammation/immunity-related genes were also increased in Ts1Rhr mice, indicating that the responsible gene(s) for this phenotype should be located among the ~30 genes in the trisomic region of Ts1Rhr mice (Supplementary Table S7), which includes the ETS transcriptional factor, ETS2. Interestingly, activation of ETS2 has been implicated in inflammation (53). To assess the role of Ets2, we disrupted the *Ets2* locus in mice to produce Ts1Cje-Ets2$^{+/+/-}$ mice by crossing Ts1Cje males and Ets2$^{+/-}$ females. Although our microarray data showed that Ets2 mRNA expression was approximately 1.3-fold higher in the brain of Ts1Cje embryos than in WT mice without a significant difference, the qRT-PCT analysis showed that the Ets2 mRNA expression was significantly increased by 1.5-fold in Ts1Cje mice (Supplementary Figure S3A). In addition, the Ets2 mRNA expression in Ts1Cje-Ets2$^{+/+/-}$ mice was comparable to that

This article is protected by copyright. All rights reserved.

Accepted Article

in WT mice, meaning that the Ets2 mRNA was expressed in a copy number-dependent manner (Supplementary Figure S3A). Although the mRNA expression of S100a8, Stfa1 and Ly6c1 tended to decrease in $Ets2^{+/-}$ mice, increases in the levels of these mRNAs were nevertheless observed in the brain of Ts1Cje-$Ets2^{+/+/-}$ embryos (Figure 4A-C), indicating that a gene(s) in the Ts1Rhr trisomic region other than the *Ets2* gene is involved in the increased expression of inflammation/immunity-related genes in the embryonic brain of DS model mice.

We focused next on another ETS transcription factor, Erg, which is also located in the trisomic region of Ts1Rhr mice. It has been demonstrated that Erg mRNA is expressed predominantly in mesodermal tissues, including vascular endothelial cells, precartilaginous and urogenital areas, as well as in migrating neural crest cells in mouse embryo (51) and that ERG protein is predominantly expressed in the nuclei of endothelial cells in mouse embryo (2). Consistently, we also confirmed that the expression was in the nuclei of vascular endothelial cells but not brain macrophages, including microglia and intrinsic immune cells, by immunohistochemistry using E14.5 mouse brain sections (Supplementary Figure S4). Using mice carrying the non-functional Erg^{Mld2} allele (34), we produced Ts1Cje-$Erg^{+/+/Mld2}$ mice that are disomic for functional Erg but otherwise trisomic on a Ts1Cje background by crossing Ts1Cje males and $Erg^{+/Mld2}$ females. Importantly, the increased mRNA expression of S100a8 and Stfa1 in Ts1Cje mice was significantly reduced in Ts1Cje-$Erg^{+/+/Mld2}$ mice

This article is protected by copyright. All rights reserved.

Accepted Article

in comparison to Ts1Cje mice (Figure 4D-F), whereas the expression of Ly6c1 mRNA varied relatively little among these mice. These results indicate that the triplication of the *Erg* gene, but not *Ets2* gene, increases the expression of inflammation/immunity-related genes.

Triplication of the Erg gene causes an increased ratio of inflammatory cells in the brain of Ts1Cje embryos

In addition to S100a8, A100a9 and Ly6c1, our microarray analysis showed that the expression level of myeloperoxidase (MPO) was also increased in the brain of Ts1Cje embryos. This enzyme is known to be abundantly expressed in neutrophils and monocytes (28). We hypothesized that the higher expression of such immune gene was due to the recruitment of higher number of immune cells in the embryonic brain of Ts1Cje mice in comparison to WT mice. Hence, we performed flow cytometry on brain cell suspensions from embryos of WT, Ts1Cje, Ts1Cje-Erg$^{+/+/Mld2}$ and Erg$^{+/Mld2}$ mice. As shown in Figure 5, the relative numbers of neutrophils (defined as CD45^{+}, CD11b^{+}, F4/80^{lo}, Ly6C^{+}, Ly6G^{+}; fraction c) and monocytes (CD45^{+}, CD11b^{+}, F4/80^{lo}, Ly6C^{+}, Ly6G^{-}; fraction b) in the brain of Ts1Cje mice were increased compared to those in WT mice (Figure 5). In contrast, such increment in relative number was significantly reduced in Ts1Cje-Erg$^{+/+/Mld2}$ mice in comparison to those in Ts1Cje mice,

This article is protected by copyright. All rights reserved.

Accepted Article

suggesting that triplication of *Erg* gene is related to the increase in relative numbers of neutrophils and monocytes in the brain of Ts1Cje embryos. The relative numbers of CD45-positive cells in the living cells were comparable, regardless of genotype, although there was significantly difference between Ts1Cje-Erg$^{+/+/Mld2}$ mice and Erg$^{Mld2/+}$ mice (WT [n = 5], 0.61 ± 0.068%; Ts1Cje [n = 5], 0.69 ± 0.068%; Ts1Cje-Erg$^{+/+/Mld2}$ [n = 5], 0.74 ± 0.060%; Erg$^{Mld2/+}$ [n = 5], 0.56 ± 0.027%, $p < 0.05$; Ts1Cje-Erg$^{+/+/Mld2}$ vs. Erg$^{Mld2/+}$ mice). In addition, the relative number of brain macrophages, defined as CD45^{+}, F4/80^{+}, CD11b^{+} cells (Figure 5A, population a), which consist of microglia, a major resident macrophages in the brain, and macrophages in the meningeal and perivascular areas (17), decreased in Ts1Cje mice compared to WT mice, whereas those numbers in Ts1Cje-Erg$^{+/+/Mld2}$ mice were comparable to those in WT mice (Figure 5B, fraction a). To distinguish the meningeal macrophages on the brain surface and microglia and perivascular macrophages inside the brain, we further carried out immunohistochemistry with an anti-F4/80 antibody. The density of F4/80-positive macrophages inside the brain, in the cerebral cortex, of Ts1Cje mice were significantly lower than that in WT and Ts1Cje-Erg$^{+/+/Mld2}$ mice (Figure 6A, B). Therefore, we conclude that the number of brain macrophages excluding meningeal macrophages decreased in the brain of Ts1Cje embryos.

This article is protected by copyright. All rights reserved.

Accepted Article

Accepted Article

Altogether, our results suggest that the triplication of the *Erg* gene is responsible for not only the increased relative numbers of recruited neutrophils and monocytes but also the decreased relative number of brain macrophages, including developmental microglia and/or perivascular macrophages. Additionally, the morphological complexity of the brain macrophages, which is an indicator of microglial branching (ramified form), in the Ts1Cje embryos seemed to be lower in comparison to WT controls and Ts1Cje-Erg $^{+/+/Mld2}$ mice (Figure 6C). Thus, a morphological analysis, taking into account cell circularity analysis, was performed as previously published (46). This revealed that Ts1Cje brain macrophages were more circular than those in WT mice, whereas the circularity of Ts1Cje-Erg$^{+/+/Mld2}$ brain macrophages was closer to that of WT mice (Figure 6D). These results indicated that inflammatory amoeboid-type brain macrophages may be dominant in *Erg*-triplicated Ts1Cje mice, in line with inflammatory mRNA profile changes in relative immune cell numbers.

Decreased cortical neurogenesis in Ts1Cje embryos is dependent on the dosage of the Erg gene

Prenatal pro-inflammation may induce the reduction of embryonic neurogenesis in mice (48). Thus, we assessed the prenatal neurogenesis in Ts1Cje-Erg$^{+/+/Mld2}$ vs Ts1Cje-Erg$^{+/+/+}$ mice to evaluate the effects of *Erg* triplication on the impaired prenatal neurogenesis in Ts1Cje mice on E14.5 (25).

This article is protected by copyright. All rights reserved.

Accepted Article

Pregnant Ts1Cje females were injected with 5-bromo-2'-deoxyuridine (BrdU) on E13.5, and the prenatal neurogenesis 24 h later was assessed by counting the number of $BrdU^{+}Ki67^{-}$ cells, which are differentiated into neurons by exiting cell cycle. Importantly, the decreased neurogenesis in Ts1Cje embryos was restored to normal level in Ts1Cje- $Erg^{+/+/Mld2}$ mice (Figure 7A-C). In addition, we also found increased number of cells expressing Tbr2 (a marker of basal progenitors) in Ts1Cje mice, whereas the number of Tbr2-positive cells in the developing neocortex of Ts1Cje-$Erg^{+/+/Mld2}$ mice was lower than that of Ts1Cje mice (Figure 7D and 7E), suggesting that in Ts1Cje embryos, differentiation into neurons was suppressed by triplication of *Erg* gene. These results suggest that triplication of the *Erg* gene causes the delayed cortical development in Ts1Cje embryos.

DISCUSSION

In the present study, DNA microarray analysis of E14.5 Ts1Cje embryo brain revealed elevated expression of S100a8, S100a9, MPO, and Ly6c1 mRNAs, which are abundant in neutrophils and/or monocytes (28, 15). Our flow cytometry analysis also demonstrated that increased relative numbers of neutrophils ($CD45^{+}$, $CD11b^{hi}$, $F4/80^{lo}$, $Ly6C^{+}$, $Ly6G^{+}$) and monocytes ($CD45^{+}$, $CD11b^{hi}$, $F4/80^{lo}$, $Ly6C^{+}$, $Ly6G^{-}$) were detected in the brain of Ts1Cje embryos. We also showed that the relative

This article is protected by copyright. All rights reserved.

number of brain macrophages ($CD45^+$, $F4/80^+$, $CD11b^+$), including developmental microglia and/or perivascular macrophages, in Ts1Cje embryos was significantly decreased compared to that in WT mice, unlike the neutrophils and monocytes. In addition, the '*in vivo* genetic subtraction approach' using Ts1Cje-$Erg^{+/Mld2}$ mice revealed that the increased gene-dose of *Erg* is responsible for the increase in the relative number of inflammatory cells and the decrease in the relative number of brain macrophages. Finally, the '*in vivo* BrdU-labeling experiment' demonstrated that triplication of the *Erg* gene caused the decreased cortical neurogenesis in the Ts1Cje embryos at E14.5. These data reveal, for the first time, that increased gene dosage of *Erg* gene in a mouse model of DS is largely responsible for the disturbed distribution of immune-related cells and embryo neurogenesis.

In this study, the microarray analysis of the brain of Ts1Cje mice at E14.5 revealed that the expression of many transcripts coded in the disomic genome are dysregulated in addition to the over-expression of genes in the trismic region. Among the transcripts dysregulated in the disomic region, the expression of inflammation/immunity-related transcripts (including S100a8 and S100a9) is especially upregulated. Similarly, the expression of S100a8 and S100a9 mRNA in the fetal liver of Ts1Cje mice was shown to be upregulated in comparison to WT mice at E14.5 (37). Another microarray study using the brain of Ts1Cje mice at E15.5 also revealed the altered expression of a number of genes coded outside the trisomic region; however, the expression of genes related to

This article is protected by copyright. All rights reserved.

Accepted Article

inflammation was not noted in the study (18). Thus, a number of genes coded outside the trisomic region seem to be deregulated in the fetal organs of Ts1Cje mice. In contrast, our previous study has shown that genes that are overexpressed in the brain of neonatal Ts1Cje mice are primarily located on the trisomic region, and that very few genes are differentially expressed outside the trisomic region (1). We also showed the disturbed expression of proteins in the prenatal brain—but not the neonatal brain—of Ts1Cje mice in a comparative proteomics analysis (26). These observations may indicate that different changes in the expression of genes coded in the disomic region are induced by the overexpression of genes encoded in the trisomic region in the brain of Ts1Cje mice during prenatal and postnatal life.

In the present study, we exclusively analyzed male mice, as we have already described some postnatal abnormal phenotypes, including behavior tests, in adult Ts1Cje males (25, 44). Maternal restraint stress has been shown to impair the acquisition of spatial learning in male rats but not in females for the Morris water maze test (59), suggesting the different levels of sensitivity for male and female rodents to the effects of prenatal stress on spatial learning. Furthermore, the effects of prenatal exposure of the neurotoxicant lead (Pb), which alters brain development, on some postnatal behaviors, such as aggressive behavior and anxiety-related behavior, differ between males and females (27). We

This article is protected by copyright. All rights reserved.

Accepted Article

therefore expected the abnormal phenotypes of prenatal brains in Ts1Cje males to differ from those in females.

Flow cytometry of the brain of Ts1Cje embryos revealed an increase in the relative number of neutrophils and monocytes in the brain of Ts1Cje embryos, and we further demonstrated that this increased ratio in CD45-positive cells was dependent on of the *Erg* gene dosage. Trafficking of immune cells into the central nervous system is a typical feature of cerebral inflammatory diseases (21, 23). The recruitment of inflammatory cells into the brain parenchyma may also be increased in DS and consequently induce inflammation. Supporting the hypothesis regarding elevated inflammation in the brain of Ts1Cje embryos, the morphological analysis revealed that a number of brain macrophages were round in shape, which is suggestive of activation, in Ts1Cje embryos. Additionally, S100a8 and S100a9, which were annotated as upregulated genes in Ts1Cje mice on our microarray, are known as members of the damage-associated molecular pattern molecules playing a role in initiating and promoting inflammation (13). It is of interest that S100a9 expression is necessary for recruitment of neutrophils to the brain (11). These facts suggest that the promoted infiltration of inflammatory cells may elevate the inflammation in the brain of Ts1Cje mice. If so, how does the *Erg* gene dosage affect the recruitment of inflammatory cells? Based on the predominant expression of Erg in endothelial cells, it is easy to infer that the overexpression of Erg may affect the function of

This article is protected by copyright. All rights reserved.

Accepted Article

endothelial cells such as vascular permeability. However, Erg has been shown to promote the expression of vascular endothelial cadherin (VE-cadherin), which is the major component of the endothelial adherens junctions (4). The expression of this adhesion molecule affects vascular permeability (8). Thus, the overexpression of Erg is assumed to consolidate the tight junctions of vascular endothelial cells, promoting the expression of VE-cadherin. It is of noteworthy that the function of VE-cadherin on vascular permeability is regulated by not only its expression level but also the posttranslational modification. It has been shown that phosphorylation of VE-cadherin results in the internalization of VE-cadherin from the adherens junctions and the subsequent loss of the endothelial barrier function (9).

In this study, we also found that the relative number of brain macrophages in Ts1Cje embryos was significantly decreased in an *Erg* gene dosage-dependent manner, in contrast to the increase in the relative number of neutrophils and monocytes. Apart from the role of *Erg* in the endothelial cells, it has been shown that *Erg* plays a role in the self-renewal of hematopoietic stem cells (HSCs) and hematopoiesis in the liver during embryogenesis (47, 55). In addition, a deficiency of *Erg* gene in the HSCs results in the loss of myeloid cells in adult mice (29). Based upon the Erg function of HSCs, during embryogensis, the number of HSCs may be increased in Ts1Cje mice with 3 copies of the *Erg* gene. In fact, the proportion of granulocyte-macrophage progenitors is increased in number, although

This article is protected by copyright. All rights reserved.

Accepted Article

the number of common myeloid progenitors is decreased in the bone marrow of Ts1Cje adults (5), suggesting that the differentiation of HSCs toward the granulocytic lineage might be specifically enhanced in Ts1Cje mice. However, the brain macrophages are suggested to be differentiated from more cell types than just HSCs; for examples, the progenitors of microglia, a major population of brain macrophage, are erythro-myeloid progenitors (EMPs)-derived yolk sac macrophages that do not pass through a monocytic intermediate stage (16). Although we could not distinguish the developmental microglia and perivascular macrophages in brains of Ts1Cje mice, the decrease in the relative number of brain macrophages may be caused by the dysregulation in the number of the progenitors for brain macrophages. A future study of the Erg effects on the maintenance of brain macrophage progenitors such as EMPs may provide further insight. Of course, it is possible that increase in the number of monocytes with the decrease in the number of brain macrophages may simply be due to inhibition of differentiation from monocytes to perivascular macrophages in the brain of Ts1Cje mice by the triplication of the *Erg* gene.

We have shown here that Ts1Cje-Erg$^{+/+/Mld2}$ mice exhibit improved prenatal neurogenesis in the cortex in contrast to the decreased cortical neurogenesis that is observed in Ts1Cje embryos, indicating that the triplication of the *Erg* gene causes reduced cortical neurogenesis in the fetal brain of Ts1Cje mice. We also showed that the number of brain macrophages in the E14.5 brain of Ts1Cje

This article is protected by copyright. All rights reserved.

Accepted Article

mice was significantly decreased in comparison to WT mice. Recently, microglia, a major population of brain macrophages, have been suggested to play a role in successful brain development and wiring through their involvement in a number of physiological processes, including developmentally regulated neuronal apoptosis, neurogenesis and synaptic pruning (36, 43, 45, 52). Since the decreased density of brain macrophages was not detected in Ts1Cje-Erg$^{+/+/Mld2}$ mice, it is conceivable that the triplication of *Erg* gene reduces cortical neurogenesis in the prenatal developing brain through the reduction in the relative number of brain macrophages. Can the triplication of *Erg* gene explain the impairment of neurogenesis in the cerebral cortex of embryos with DS? RNA interference by *in utero* electroporation experiments have revealed that increasing the dosage of dual-specificity tyrosine-phosphorylated and -regulated kinase 1A (*Dyrk1a*) and regulator of calcineurin 1 (*Rcan1*), which are coded within trisomic region of Ts1Cje mice, in neural progenitors leads to a delay in neuronal differentiation by the deregulation of a nuclear factor of activated T-cells, cytoplasmic 4 (NFATc4) (32). However, the rigorous gene dosage effects of *Dyrk1a* and *Rcan1* genes have never been assessed using knockout mice. In the present study, we clearly showed that the dosage of the *Erg* gene disturbed the neonatal neurogenesis in Ts1Cje mice, suggesting that the increased expression of *Erg* is also involved in the defective neurogenesis in the prenatal cortex of Ts1Cje mice. Although the functional interaction between Erg and NFATc4 has remained unknown, the elucidation of the cross-

This article is protected by copyright. All rights reserved.

Accepted Article

talk between these molecules may provide a new insight into the mechanism underlying the delayed brain development of individuals with DS.

In this study, we found that in the fetal brain of Ts1Cje mice, the relative number of neutrophils and monocytes was increased and the relative number of brain macrophages was decreased by an increase in the *Erg* gene dosage. Additionally, the increased expression of Erg necessarily contributes to the impaired prenatal neurogenesis in Ts1Cje mice. Taken together, the *Erg* gene would be an important target gene for pharmacotherapy targeting the brain developmental delay associated with the defective prenatal cortical neurogenesis in individuals with DS. We previously demonstrated a number of abnormal behaviors in Ts1Cje adults, including cognitive impairment (41), environmental stimuli-triggered hyperactivity, increased sociability and decreased depression-like behavior (44). Examining the association of impaired cortical neurogenesis and disturbances in populations of immune cells in Ts1Cje embryos with postnatal abnormal behaviors using Ts1Cje-Erg$^{+/+/Mld2}$ mice might help establish a way to improve certain abnormalities in people with DS during pregnancy.

This article is protected by copyright. All rights reserved.

ACKNOWLEDGEMENTS

We are grateful to F. Tsushimi, S. Sugimoto, A. Izumoto, S. Wakigi, A. Nakano, (Dept. of Pathol. Biochem.) and K. Kaneda (Dept. of Clin. Transl. Physiol.) at Kyoto Pharmaceutical University for assistance in the bioinfomatics analysis, and immunohistochemistry. We are also thankful for the help of S. Mifsud, The Walter and Eliza Hall Institute of Medical Research for transporting the $Erg^{Mld2/+}$ mice. F.G. is an EMBO YIP awardee.

FOOT NOTE

Gene Expression Omnibus Dataset: Data have been uploaded to the GEO site and made publically available (GEO accession: GSE121449).

Competing interests: The authors declare that no competing interests exist.

AUTHOR CONTRIBUTIONS

K.I. designed and carried out the experiments, analyzed the data, wrote the manuscript and provided financial support. K.A., A.S. and K.Y. contributed to the generation of the *Ets2* knockout model. K.T.,

This article is protected by copyright. All rights reserved.

Accepted Article

D.L., T.N. and F.G. performed the FACS analysis, discussed the results and wrote the manuscript. R.S., E.K. and S.A. performed experiments and commented on the manuscript. W.A. provided advice and the *Mld2* mouse model and wrote the manuscript. H.S. discussed the results and commented on the manuscript.

FUNDING

This study was supported in part by grants from Takeda Science Foundation (2016) (to K.I.), the JSPS KAKENHI Grant Numbers 18K06940 (to K.I.), the Vehicle Racing Commemorative Foundation (2017) (to K.I.), Kyoto Pharmaceutical University Fund for the Promotion of Scientific Research (to K.I.), Fellowship (1058344) and Program Grant (1113577) from the Australian National Health and Medical Research Council (to W.A.) and Singapore Immunology Network (SIgN) core funding as well as a Singapore National Research Foundation Senior Investigatorship (NRFI) NRF2016NRF-NRFI001-02 (to F.G.).

This article is protected by copyright. All rights reserved.

Accepted Article

Accepted Article

REFERENCES

1. Amano K, Sago H, Uchikawa C, Suzuki T, Kotliarova SE, Nukina N, Epstein CJ, Yamakawa K (2004) Dosage-dependent over-expression of genes in the trisomic region of Ts1Cje mouse model for Down syndrome. Hum Mol Genet 13:1333-1340.

2. Arnold TD, Niaudet C, Pang MF, Siegenthaler J, Gaengel K, Jung B, Ferrero GM, Mukouyama YS, Fuxe J, Akhurst R, Betsholtz C, Sheppard D, Reichardt LF (2014) Excessive vascular sprouting underlies cerebral hemorrhage in mice lacking alphaVβ8-TGFβ signaling in the brain. Development 141:4489-4499.

3. Belichenko NP, Belichenko PV, Kleschevnikov AM, Salehi A, Reeves RH, Mobley WC (2009) The "Down syndrome critical region" is sufficient in the mouse model to confer behavioral, neurophysiological, and synaptic phenotypes characteristic of Down syndrome. J Neurosci 29:5938-5948.

4. Birdsey GM, Dryden NH, Amsellem V, Gebhardt F, Sahnan K, Haskard DO, Dejana E, Mason JC, Randi AM (2008) Transcription factor Erg regulates angiogenesis and endothelial apoptosis through VE-cadherin. Blood 111:3498-3506.

This article is protected by copyright. All rights reserved.

Accepted Article

5. Carmichael CL, Majewski IJ, Alexander WS, Metcalf D, Hilton DJ, Hewitt CA, Scott HS (2009) Hematopoietic defects in the Ts1Cje mouse model of Down syndrome. Blood 113:1929-1937.

6. Chakrabarti L, Galdzicki Z, Haydar TF (2007) Defects in embryonic neurogenesis and initial synapse formation in the forebrain of the Ts65Dn mouse model of Down syndrome. J Neurosci 27:11483-11495.

7. Davisson MT, Schmidt C, Akeson EC (1990) Segmental trisomy of murine chromosome 16: a new model system for studying Down syndrome. Prog Clin Biol Res 360:263-280.

8. Dejana E, Orsenigo F (2013) Endothelial adherens junctions at a glance. J Cell Sci 126:2545-2549.

9. Dejana E, Orsenigo F, Lampugnani MG (2008) The role of adherens junctions and VE-cadherin in the control of vascular permeability. J Cell Sci 121:2115-2122.

10. Dennis G, Jr., Sherman BT, Hosack DA, Yang J, Gao W, Lane HC, Lempicki RA (2003) DAVID: Database for Annotation, Visualization, and Integrated Discovery. Genome Biol 4:P3.

11. Denstaedt SJ, Spencer-Segal JL, Newstead MW, Laborc K, Zhao AP, Hjelmaas A, Zeng X, Akil H, Standiford TJ, Singer BH (2018) S100A8/A9 Drives Neuroinflammatory Priming and Protects against Anxiety-like Behavior after Sepsis. J Immunol 200:3188-3200.

This article is protected by copyright. All rights reserved.

Accepted Article

12. Duchon A, Raveau M, Chevalier C, Nalesso V, Sharp AJ, Herault Y (2011) Identification of the translocation breakpoints in the Ts65Dn and Ts1Cje mouse lines: relevance for modeling Down syndrome. Mamm Genome 22:674-684.

13. Ehrchen JM, Sunderkotter C, Foell D, Vogl T, Roth J (2009) The endogenous Toll-like receptor 4 agonist S100A8/S100A9 (calprotectin) as innate amplifier of infection, autoimmunity, and cancer. J Leuk Biol 86:557-566.

14. Epstein CJ (2001) Down syndrome (trisomy 21). In: The Metabolic and Molecular Bases Inherited Disease 8th edn, Scriver CR, Beaudet, A. L., Sly, W. S., Valle, D., (eds.), pp. 1223-1256, McGraw Hill Education: New York.

15. Gebhardt C, Nemeth J, Angel P, Hess J (2006) S100A8 and S100A9 in inflammation and cancer. Biochem Pharmacol 72:1622-1631.

16. Ginhoux F, Greter M, Leboeuf M, Nandi S, See P, Gokhan S, Mehler MF, Conway SJ, Ng LG, Stanley ER, Samokhvalov IM, Merad M (2010) Fate mapping analysis reveals that adult microglia derive from primitive macrophages. Science 330:841-845.

17. Goldmann T, Wieghofer P, Jordao MJ, Prutek F, Hagemeyer N, Frenzel K, Amann L, Staszewski O, Kierdorf K, Krueger M, Locatelli G, Hochgerner H, Zeiser R, Epelman S, Geissmann F, Priller

This article is protected by copyright. All rights reserved.

Accepted Article

J, Rossi FM, Bechmann I, Kerschensteiner M, Linnarsson S, Jung S, Prinz M (2016) Origin, fate and dynamics of macrophages at central nervous system interfaces. Nat Immunol 17:797-805.

18. Guedj F, Pennings JL, Ferres MA, Graham LC, Wick HC, Miczek KA, Slonim DK, Bianchi DW (2015) The fetal brain transcriptome and neonatal behavioral phenotype in the Ts1Cje mouse model of Down syndrome. Am J Med Genet A 167a:1993-2008.

19. Guedj F, Pennings JL, Wick HC, Bianchi DW (2015) Analysis of adult cerebral cortex and hippocampus transcriptomes reveals unique molecular changes in the Ts1Cje mouse model of down syndrome. Brain Pathol 25:11-23.

20. Haydar TF, Reeves RH (2012) Trisomy 21 and early brain development. Trend Neurosci 35:81-91.

21. Hemmer B, Cepok S, Zhou D, Sommer N (2004) Multiple sclerosis -- a coordinated immune attack across the blood brain barrier. Curr Neurovasc Res 1:141-150.

22. Huang da W, Sherman BT, Lempicki RA (2009) Systematic and integrative analysis of large gene lists using DAVID bioinformatics resources. Nat Protocol 4:44-57.

23. Hult B, Chana G, Masliah E, Everall I (2008) Neurobiology of HIV. Int Rev Psychiatry 20:3-13.

This article is protected by copyright. All rights reserved.

Accepted Article

24. Ishihara K, Akiba S (2017) A Comprehensive Diverse '-omics' Approach to Better Understanding the Molecular Pathomechanisms of Down Syndrome. Brain Sci 7(4).

25. Ishihara K, Amano K, Takaki E, Shimohata A, Sago H, Epstein CJ, Yamakawa K (2010) Enlarged brain ventricles and impaired neurogenesis in the Ts1Cje and Ts2Cje mouse models of Down syndrome. Cereb Cortex 20:1131-1143.

26. Ishihara K, Kanai S, Sago H, Yamakawa K, Akiba S (2014) Comparative proteomic profiling reveals aberrant cell proliferation in the brain of embryonic Ts1Cje, a mouse model of Down syndrome. Neuroscience 281:1-15.

27. Kasten-Jolly J, Lawrence DA (2017) Sex-specific effects of developmental lead exposure on the immune-neuroendocrine network. Toxicol Appl Pharmacol 334:142–157.

28. Kettle AJ, Winterbourn CC (1997) Myeloperoxidase: a key regulator of neutrophil oxidant production. Redox Rep 3:3-15.

29. Knudsen KJ, Rehn M, Hasemann MS, Rapin N, Bagger FO, Ohlsson E, Willer A, Frank AK, Sondergaard E, Jendholm J, Thoren L, Lee J, Rak J, Theilgaard-Monch K, Porse BT (2015) ERG promotes the maintenance of hematopoietic stem cells by restricting their differentiation. Genes Dev 29:1915-1929.

This article is protected by copyright. All rights reserved.

30. Korenberg JR, Kawashima H, Pulst SM, Allen L, Magenis E, Epstein CJ (1990) Down syndrome: toward a molecular definition of the phenotype. Am J Med Genet Suppl 7:91-97.

31. Kudo LC, Parfenova L, Vi N, Lau K, Pomakian J, Valdmanis P, Rouleau GA, Vinters HV, Wiedau-Pazos M, Karsten SL (2010) Integrative gene-tissue microarray-based approach for identification of human disease biomarkers: application to amyotrophic lateral sclerosis. Hum Mol Genet 19:3233-3253.

32. Kurabayashi N, Sanada K (2013) Increased dosage of DYRK1A and DSCR1 delays neuronal differentiation in neocortical progenitor cells. Genes Dev 27:2708-2721.

33. Loughran SJ, Kruse EA, Hacking DF, de Graaf CA, Hyland CD, Willson TA, Henley KJ, Ellis S, Voss AK, Metcalf D, Hilton DJ, Alexander WS, Kile BT (2008) The transcription factor Erg is essential for definitive hematopoiesis and the function of adult hematopoietic stem cells. Nat Immunol 9:810-819.

34. Ng AP, Hyland CD, Metcalf D, Carmichael CL, Loughran SJ, Di Rago L, Kile BT, Alexander WS (2010) Trisomy of Erg is required for myeloproliferation in a mouse model of Down syndrome. Blood 115:3966-3969.

This article is protected by copyright. All rights reserved.

Accepted Article

35. Olson LE, Richtsmeier JT, Leszl J, Reeves RH (2004) A chromosome 21 critical region does not cause specific Down syndrome phenotypes. Science 306:687-690.

36. Paolicelli RC, Bolasco G, Pagani F, Maggi L, Scianni M, Panzanelli P, Giustetto M, Ferreira TA, Guiducci E, Dumas L, Ragozzino D, Gross CT (2011) Synaptic pruning by microglia is necessary for normal brain development. Science 333:1456-1458.

37. Pennings JL, Rodenburg W, Imholz S, Koster MP, van Oostrom CT, Breit TM, Schielen PC, de Vries A (2011) Gene expression profiling in a mouse model identifies fetal liver- and placenta-derived potential biomarkers for Down Syndrome screening. PloS One 6:e18866.

38. Raveau M, Nakahari T, Asada S, Ishihara K, Amano K, Shimohata A, Sago H, Yamakawa K (2017) Brain ventriculomegaly in Down syndrome mice is caused by Pcp4 dose-dependent cilia dysfunction. Hum Mol Genet 26:923-931.

39. Reeves RH, Irving NG, Moran TH, Wohn A, Kitt C, Sisodia SS, Schmidt C, Bronson RT, Davisson MT (1995) A mouse model for Down syndrome exhibits learning and behaviour deficits. Nat Genet 11:177-184.

40. Ruparelia A, Pearn ML, Mobley WC (2013) Aging and intellectual disability: insights from mouse models of Down syndrome. Dev Disabil Res Rev 18:43-50.

This article is protected by copyright. All rights reserved.

Accepted Article

Accepted Article

41. Sago H, Carlson EJ, Smith DJ, Kilbridge J, Rubin EM, Mobley WC, Epstein CJ, Huang TT (1998) Ts1Cje, a partial trisomy 16 mouse model for Down syndrome, exhibits learning and behavioral abnormalities. Proc Natl Acad Sci USA 95:6256-6261.

42. Schmidt-Sidor B, Wisniewski KE, Shepard TH, Sersen EA (1990) Brain growth in Down syndrome subjects 15 to 22 weeks of gestational age and birth to 60 months. Clin Neuropathol 9:181-90.

43. Shigemoto-Mogami Y, Hoshikawa K, Goldman JE, Sekino Y, Sato K (2014) Microglia enhance neurogenesis and oligodendrogenesis in the early postnatal subventricular zone. J Neurosci 34:2231-2243.

44. Shimohata A, Ishihara K, Hattori S, Miyamoto H, Morishita H, Ornthanalai G, Raveau M, Ebrahim AS, Amano K, Yamada K, Sago H, Akiba S, Mataga N, Murphy NP, Miyakawa T, Yamakawa K (2017) Ts1Cje Down syndrome model mice exhibit environmental stimuli-triggered locomotor hyperactivity and sociability concurrent with increased flux through central dopamine and serotonin metabolism. Exp Neurol 293:1-12.

45. Squarzoni P, Oller G, Hoeffel G, Pont-Lezica L, Rostaing P, Low D, Bessis A, Ginhoux F, Garel S (2014) Microglia modulate wiring of the embryonic forebrain. Cell Rep 8:1271-1279.

This article is protected by copyright. All rights reserved.

Accepted Article

46. Takata K, Kozaki T, Lee CZW, Thion MS, Otsuka M, Lim S, Utami KH, Fidan K, Park DS, Malleret B, Chakarov S, See P, Low D, Low G, Garcia-Miralles M, Zeng R, Zhang J, Goh CC, Gul A, Hubert S, Lee B, Chen J, Low I, Shadan NB, Lum J, Wei TS, Mok E, Kawanishi S, Kitamura Y, Larbi A, Poidinger M, Renia L, Ng LG, Wolf Y, Jung S, Onder T, Newell E, Huber T, Ashihara E, Garel S, Pouladi MA, Ginhoux F (2017) Induced-Pluripotent-Stem-Cell-Derived Primitive Macrophages Provide a Platform for Modeling Tissue-Resident Macrophage Differentiation and Function. Immunity 47:183-98.e6.

47. Taoudi S, Bee T, Hilton A, Knezevic K, Scott J, Willson TA, Collin C, Thomas T, Voss AK, Kile BT, Alexander WS, Pimanda JE, Hilton DJ (2011) ERG dependence distinguishes developmental control of hematopoietic stem cell maintenance from hematopoietic specification. Genes Dev 25:251-262.

48. Tronnes AA, Koschnitzky J, Daza R, Hitti J, Ramirez JM, Hevner R (2016) Effects of Lipopolysaccharide and Progesterone Exposures on Embryonic Cerebral Cortex Development in Mice. Reprod Sci 23:771-778.

49. Ulas T, Pirr S, Fehlhaber B, Bickes MS, Loof TG, Vogl T, Mellinger L, Heinemann AS, Burgmann J, Schoning J, Schreek S, Pfeifer S, Reuner F, Vollger L, Stanulla M, von Kockritz-

This article is protected by copyright. All rights reserved.

Blickwede M, Glander S, Barczyk-Kahlert K, von Kaisenberg CS, Friesenhagen J, Fischer-Riepe L, Zenker S, Schultze JL, Roth J, Viemann D (2017) S100-alarmin-induced innate immune programming protects newborn infants from sepsis. Nat Immunol 18:622-632.

50. Villar AJ, Belichenko PV, Gillespie AM, Kozy HM, Mobley WC, Epstein CJ (2005) Identification and characterization of a new Down syndrome model, Ts[Rb(12.17^{16})]2Cje, resulting from a spontaneous Robertsonian fusion between T(17^{16})65Dn and mouse chromosome 12. Mamm Genome 16:79-90.

51. Vlaeminck-Guillem V, Carrere S, Dewitte F, Stehelin D, Desbiens X, Duterque-Coquillaud M (2000) The Ets family member Erg gene is expressed in mesodermal tissues and neural crests at fundamental steps during mouse embryogenesis. Mech Develop 91:331-335.

52. Wakselman S, Bechade C, Roumier A, Bernard D, Triller A, Bessis A (2008) Developmental neuronal death in hippocampus requires the microglial CD11b integrin and DAP12 immunoreceptor. J Neurosci 28:8138-8143.

53. Wei G, Guo J, Doseff AI, Kusewitt DF, Man AK, Oshima RG, Ostrowski MC (2004) Activated Ets2 is required for persistent inflammatory responses in the motheaten viable model. J Immunology 173:1374-1379.

This article is protected by copyright. All rights reserved.

Accepted Article

54. Williams RW, Rakic P (1988) Three-dimensional counting: an accurate and direct method to estimate numbers of cells in sectioned material. J Comp Neurol 278:344-352.

55. Xie Y, Koch ML, Zhang X, Hamblen MJ, Godinho FJ, Fujiwara Y, Xie H, Klusmann JH, Orkin SH, Li Z (2017) Reduced Erg Dosage Impairs Survival of Hematopoietic Stem and Progenitor Cells. Stem cells 35:1773-1785.

56. Yamakawa K (2012) Towards the understanding of Down syndrome using mouse models. Congenit Anom 52:67-71.

57. Yamamoto H, Flannery ML, Kupriyanov S, Pearce J, McKercher SR, Henkel GW, Maki RA, Werb Z, Oshima RG (1998) Defective trophoblast function in mice with a targeted mutation of Ets2. Genes Dev 12:1315-1326.

58. Yuan P, Condello C, Keene CD, Wang Y, Bird TD, Paul SM, Luo W, Colonna M, Baddeley D, Grutzendler J (2016) TREM2 Haplodeficiency in Mice and Humans Impairs the Microglia Barrier Function Leading to Decreased Amyloid Compaction and Severe Axonal Dystrophy. Neuron 90:724-739.

59. Zagron G, Weinstock M (2006) Maternal adrenal hormone secretion mediates behavioural alterations induced by prenatal stress in male and female rats. Behav Brain Res 175:323–328.

This article is protected by copyright. All rights reserved.

Accepted Article

Accepted Article

FIGURE LEGENDS

Figure 1. The gene dose-dependent overexpression of genes in the trisomic region of the brain of Ts1Cje embryos. Genes are arranged from the proximal end (top) to the distal end (bottom) of MMU16 according to the mapping data of the NCBI Mouse Genome Resource (http://www.ncbi.nlm.nih.gov/genome/guide/mouse/). The region marked by arrows is the triplicated segment in Ts1Cje mice. The detailed information of each gene, including the gene name, the fold change value, and P-value are shown in Supplementary Tables S1 and S2.

Figure 2. The increased expression of inflammatory-related genes in Ts1Cje mice. (A) The mRNA levels, which are annotated in the microarray analysis, were validated by a real time quantitative RT-PCR. The expression of 36B4 mRNA was used as an internal control. Each value represents the mean ratio ± SEM. Statistical significance was determined with Student's *t*-test (n=5 in each genotype, $^{**}p < 0.01$, $^{***}p < 0.001$). (B) The expression levels of S100A9 and β-actin (internal control) proteins were detected by Western blotting. (C) The intensity of bands in *B* was quantified using the NIH Image J software program (developed at U.S. National Institutes of Health and available on the Internet at http://rsb.info.nih.gov/nih-image/) with a gel analysis macro. The level of

This article is protected by copyright. All rights reserved.

S100A9 protein in the fetal brain of Ts1Cje mice was significantly increased on embryonic day 14.5. Each value represents the mean ratio ± SEM. Statistical significance was determined using Student's *t*-test (n=5 in each genotype, $^{**}p < 0.01$).

Figure 3. The increased expression of inflammation/immunity-related genes in other mouse models of DS, Ts2Cje and Ts1Rhr mice. (A) Trisomic segments of DS mouse models, Ts2Cje, Ts1Cje and Ts1Rhr mice harboring partial trisomy 16 are indicated. The trisomic segment of Ts2Cje mice is equal to that of Ts65Dn mice. The number of curated protein coding genes is based on the GenBank and SwissProt databases. (B) The expression levels of genes related to inflammation and immunity, which are annotated in Figure 2A, in the embryonic brain from Ts2Cje and Ts1Rhr mice were quantified by quantitative real-time RT-PCR. Increased mRNA levels for inflammation/immunity-related genes, S100a8, S100a9, Ly6c1, Stfa1, Stfa2 and Stfa3 were conserved in both lines. The expression of 36B4 mRNA was used as internal control. Each value represents the mean ratio ± SEM. Statistical significance was determined using Student's *t*-test (WT for Ts2Cje [n = 10], Ts2Cje [n = 7], WT for Ts1Rhr [n = 12], and Ts1Rhr [n = 8]; $^{*}p < 0.05$, $^{**}p < 0.01$, $^{***}p < 0.001$, $^{****}p < 0.0001$).

This article is protected by copyright. All rights reserved.

Figure 4. The increased expression of inflammation/immunity-related genes in Ts1Cje embryos caused by the triplication of the *Erg* gene, but not *Ets2*. The S100a8, Stfa1 and Ly6c1 mRNA levels were assessed by a quantitative real-time RT-PCR. Each mRNA level was normalized with the 36B4 level. The effect of *Ets2* (A-C) or *Erg* (D-F) triplication on the increased expression of these mRNAs was examined using Ts1Cje-Ets2$^{+/+/-}$ or Ts1Cje-Erg$^{+/+/Mld2}$ mice. The data suggest that the triplication of the *Erg* gene causes the upregulation of the inflammation-related genes in the brain of Ts1Cje embryos. Each value represents mean ratio ± SEM. Statistical significance was determined using an ANOVA with an LSD post-hoc test (n = 3-4 in each genotype, respectively, $*p < 0.05$, $**p < 0.01$).

Figure 5. The ratio of immune cells in the CD45-positive cells of Ts1Cje embryo brain was disturbed by triplication of the *Erg* gene. Cells from the whole brain of WT and Ts1Cje embryos at E14.5 were stained with CD45 APC-Cy7, CD11b PE-Cy7, F4/80 APC, Ly6G FITC and Ly6C Pacific Blue antibodies. Dead cells were distinguished by staining with 7-aminoactinomycin D. In Ts1Cje mice, the relative numbers of CD45$^+$, CD11b$^+$, F4/80^{lo}, Ly6c^{int}, Ly6G$^+$ (neutrophils) and CD45$^+$, CD11b$^+$, F4/80^{lo}, Ly6c^{int}, and Ly6G$^-$ (monocytes) were significantly increased, whereas the decreased relative number of CD45$^+$, F4/80$^+$, CD11b$^+$ cells (brain macrophages) was detected. (A) Flow

This article is protected by copyright. All rights reserved.

cytometry of immune cells in fetal brain from WT, Ts1Cje, Ts1Cje-Erg$^{+/+/Mld2}$, and Erg$^{+/Mld2}$ mice. Leukocytes in the brain were defined by gating on CD45-positive cells (left panels). Brain macrophages were identified as CD45^{+} F4/80^{+} CD11b^{+} (populations a). Monocytes and neutrophils were identified as CD45^{+} CD11b^{+} F4/80^{lo} Ly6C^{+} Ly6G^{-} (population b) and CD45^{+} CD11b^{+} F4/80^{lo} Ly6C^{+} Ly6G^{+} (population c), respectively. (B) The percentage of each population within CD45^{+} cells is shown for brains from WT, Ts1Cje, Ts1Cje-Erg$^{+/+/Mld2}$ and Erg$^{+/Mld2}$ mice. Data are presented as the mean ± SEM (n = 5 mice in each genotype). Statistical significance was determined by an ANOVA with an LSD post-hoc test. $^{**}p < 0.01$

Figure 6. The density of brain macrophages in Ts1Cje embryos is decreased by triplication of the *Erg* gene. (A) Brain macrophages in WT, Ts1Cje and Ts1Cje/Erg$^{+/+/Mld2}$ mice at E14.5 were detected by immunohistochemistry with anti-F4/80 antibody (red). Nuclei were stained with DAPI (blue). Scale bars: 200 μm. (B) The F4/80-positive brain macrophages including microglia and/or perivascular macrophages inside brains but not meningeal macrophages on the surface of the cerebral cortex were counted in a blinded manner, showing that the density of microglia and/or perivascular macrophages in Ts1Cje mice is significantly decreased in comparison to the WT mice, whereas that in Ts1Cje-Erg$^{+/+/Mld2}$ mice is comparable to that in WT mice. The data are presented as the mean ± SEM

This article is protected by copyright. All rights reserved.

Accepted Article

(n = 3 mice in each genotype). (C, D) Circularity of the microglia and/or perivascular macrophages was assessed by a morphological analysis with the Image J software program. The typical morphology of F4/80-positive microglia and/or perivascular macrophages in the cerebral cortex (C) and the circularity (D) indicate that the microglia and/or perivascular macrophages in the cerebral cortex of Ts1Cje mice are activated in comparison to WT and Ts1Cje-Erg$^{+/+/Mld2}$ mice. Scale bars: 10 μm. Statistical significance was determined by an ANOVA with an LSD post-hoc test. (*$p < 0.05$, **$p < 0.01$).

Figure 7. Prenatal neurogenesis in the cerebral cortex of Ts1Cje embryos is impaired by triplication of the *Erg* gene. One pulse of 50 mg/kg BrdU was administered to pregnant Ts1Cje females on gestational day 13 (E13.5), and BrdU-positive cells at 24 h after injection were detected by immunohistochemistry. (A) Double-staining images of the cortical wall for Ki67 (red) and BrdU (green) taken at the midpoint between the medial and lateral angles of the LV show that fewer Ki67-negative/BrdU-positive cells (exiting the cell cycle) were detected in WT, Ts1Cje and Ts1Cje-Erg$^{+/+/Mld2}$ mice. Nuclei were stained with DAPI (blue). Upper panels show an image of the whole brain. Scale bar: 1 mm. Lower panels show magnified images of the cerebral cortex in the boxed area of the respective upper panel. Scale bar: 200 μm. (B) The numbers of cells exiting the cell cycle

This article is protected by copyright. All rights reserved.

Accepted Article

Accepted Article

($BrdU^+/Ki67^-$) were counted in a counting box (150 × 180 × 25 μm) in a blinded manner, demonstrating that the number of $BrdU^+/Ki67^-$ cells was reduced in embryonic cortices of Ts1Cje mice, whereas no decreased neurogenesis was detected in Ts1Cje-$Erg^{+/+/Mld2}$ mice. Values indicate the ratio of BrdU(+)/Ki67(-) cell to the total cell number in a counting box (WT [n= 10], Ts1Cje [n = 9], and Ts1Cje-$Erg^{+/+/Mld2}$ [n = 8], mean ± SEM). (C) Estimates of BrdU(+)/Ki67(-) cell numbers in the cerebral cortex were obtained using stereological cell counting. Values indicate the number of BrdU(+)/Ki67(-) cell ($\times 10^5$) per unit volume (n = 3 in each genotype, mean ± SEM). (D) The brain sections were immunostained with anti-Tbr2 antibody and counterstained with Hematoxylin. (E) Tbr2-positive cells were counted in the blinded manner. The ratio of $Tbr2^+$ cells to the total number of cortical cells is shown. In comparison to WT mice, a significant increase in the ratio of $Tbr2^+$ cells was detected in Ts1Cje mice but not in Ts1Cje-$Erg^{+/+/Mld2}$ mice. The data are presented as the mean ± SEM (n = 3 mice in each genotype). Statistical significance was determined by an ANOVA with an LSD post-hoc test $*p < 0.05$ (significantly different).

This article is protected by copyright. All rights reserved.

Accepted Article

FIGURE LEGENDS FOR SUPPLEMENTARY FIGURES

Supplementary Figure S1. The generation of Ets2-deficient mice. (A) Structure of the targeting vector. The pgk-neo cassette was inserted into the region from exon 8 to exon 10 of the *Ets2* gene. (B) Validation of recombination was performed using a PCR. The positions of the PCR primers used are indicated by arrows.

Supplementary Figure S2. The expression of genes in the monosomic region of MMU12 in Ts1Cje mice. (A) The monosomic region in Ts1Cje mice is located at the distal end of MMU12 due to translocation of a partial MMU16. The monosomic region contains five genes, *Sp4, Sp8, Abcb5, Itgb8, Macc1* and *Tmem196*, and the 3' side of the *Dnahc11* gene. (B) The expression of transcripts coded in the monosomic region of the brain of Ts1Cje embryos at E14.5 on the microarray analysis. The expression of Dnahc11 has already been shown to be increased on the 5' side of this gene product by the deletion of the 3' side of this gene (Guedj F et al., *Brain Pathol.* **25:**11–23 [2015]). In the fetal brains of WT and Ts1Cje mice, the expression levels of Sp4, Sp8 and Itgb8 mRNA were, as expected, in Ts1Cje mice in a gene-dosage dependent manner, whereas Abcb5 and Macc1 mRNA were expressed at a level that was below the limit of detection. (C) Expression of Dnahc11 and Itg8 in other

This article is protected by copyright. All rights reserved.

mouse models, Ts2Cje and Ts1Rhr mice was assessed by a quantitative real-time RT-PCR. The altered expression observed in Ts1Cje mice failed to be detected in these mouse model lines, suggesting that the abnormal expression of these genes was caused by the monosomic region of Ts1Cje mice.

Supplementary Figure S3. The expression of Ets2 and Erg mRNA in Ts1Cje-Ets2$^{+/+/-}$ and Ts1Cje-Erg$^{+/+/Mld2}$ mice, respectively. (A) The expression levels of Ets2 mRNA in embryonic brains from WT, Ts1Cje, Ets2$^{+/-}$ and Ts1Cje-Ets2$^{+/+/-}$ mice were assessed by a quantitative real-time RT-PCR. 36B4 was used as an internal control. As expected, the increased expression of Ets2 mRNA in Ts1Cje mice was restored to the control level in the Ts1Cje-Ets2$^{+/+/-}$ mice. (B) The Erg mRNA expression was also assessed by a quantitative real time RT-PCR. Since the mutant allele of Erg$^{+/Mld2}$ mice expresses Erg mRNA with a point mutation, the reduced level of Erg mRNA was not observed in Erg$^{+/Mld2}$ mice. Each value represents the mean ± SEM (arbitrary units). Statistical significance was determined by an ANOVA with an LSD post-hoc test. (n=5 in each genotype, $*p < 0.05$ $**p < 0.01$).

This article is protected by copyright. All rights reserved.

Supplementary Figure S4. Confirmation of the expression of ERG in the endothelial cells of the mouse brain at embryonic day 14.5. ERG (green) and CD31, a marker of endothelial cells (red) in the brain of WT mice on E14.5 was detected by immunohistochemistry. In line with previous reports, ERG is expressed in the nuclei of the endothelial cells. Scale bars: 200 μm.

Accepted Article

This article is protected by copyright. All rights reserved.

Accepted Article

Fig. 1 Ishihara et al.

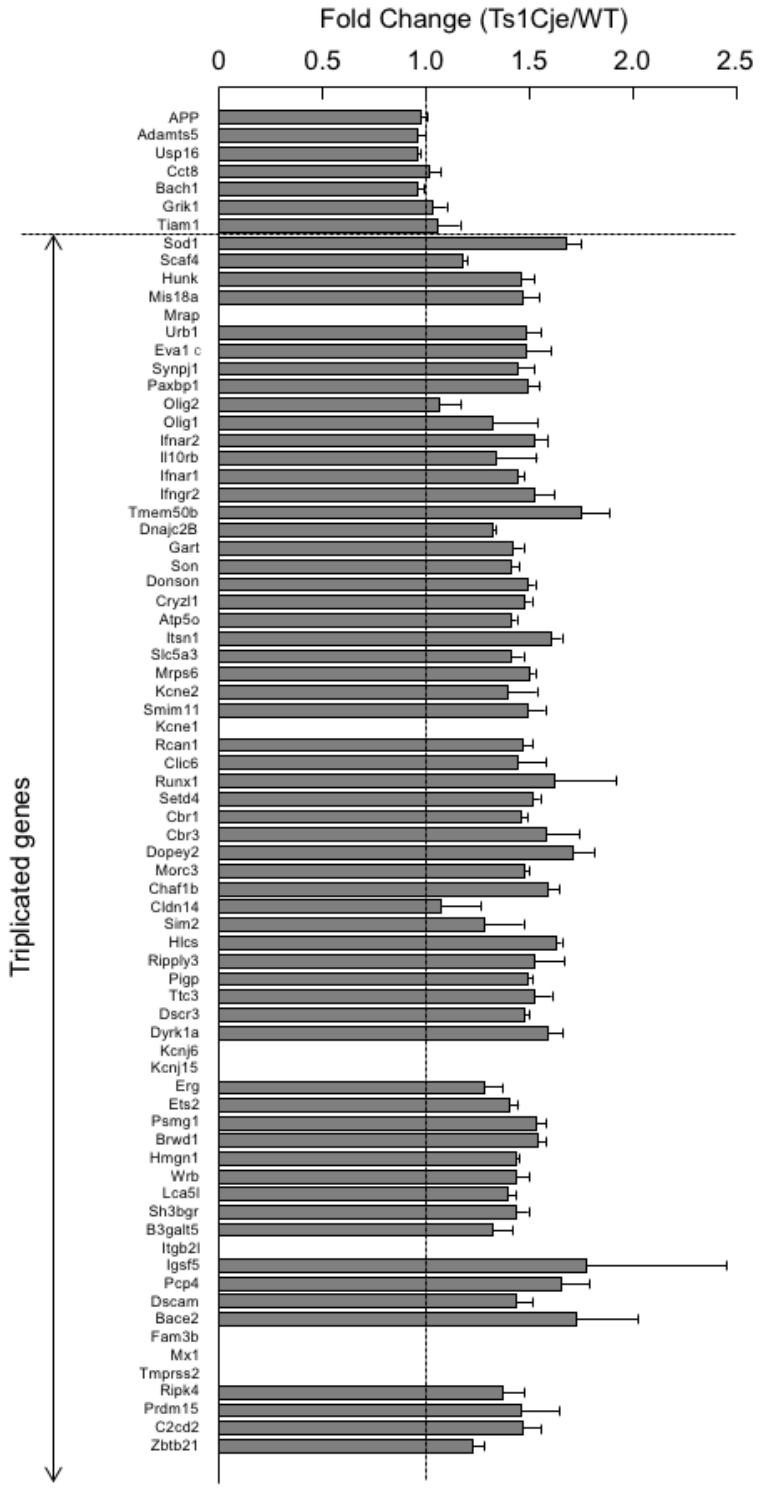

This article is protected by copyright. All rights reserved.

Accepted Article

Fig. 2 Ishihara et al.

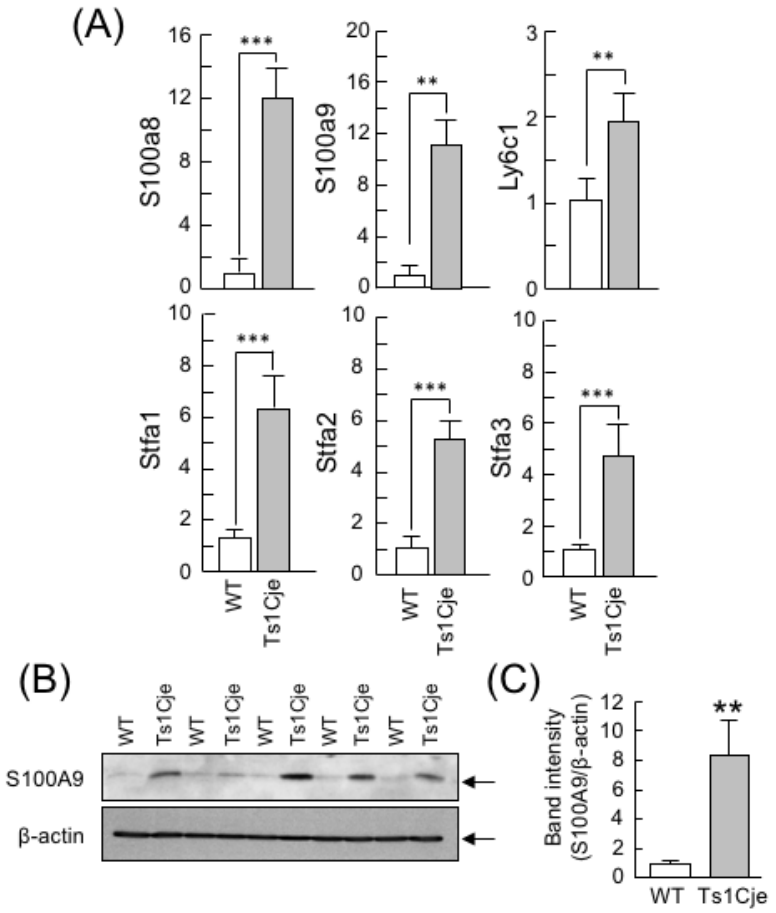

This article is protected by copyright. All rights reserved.

Accepted Article

Ishihara_Fig. 3

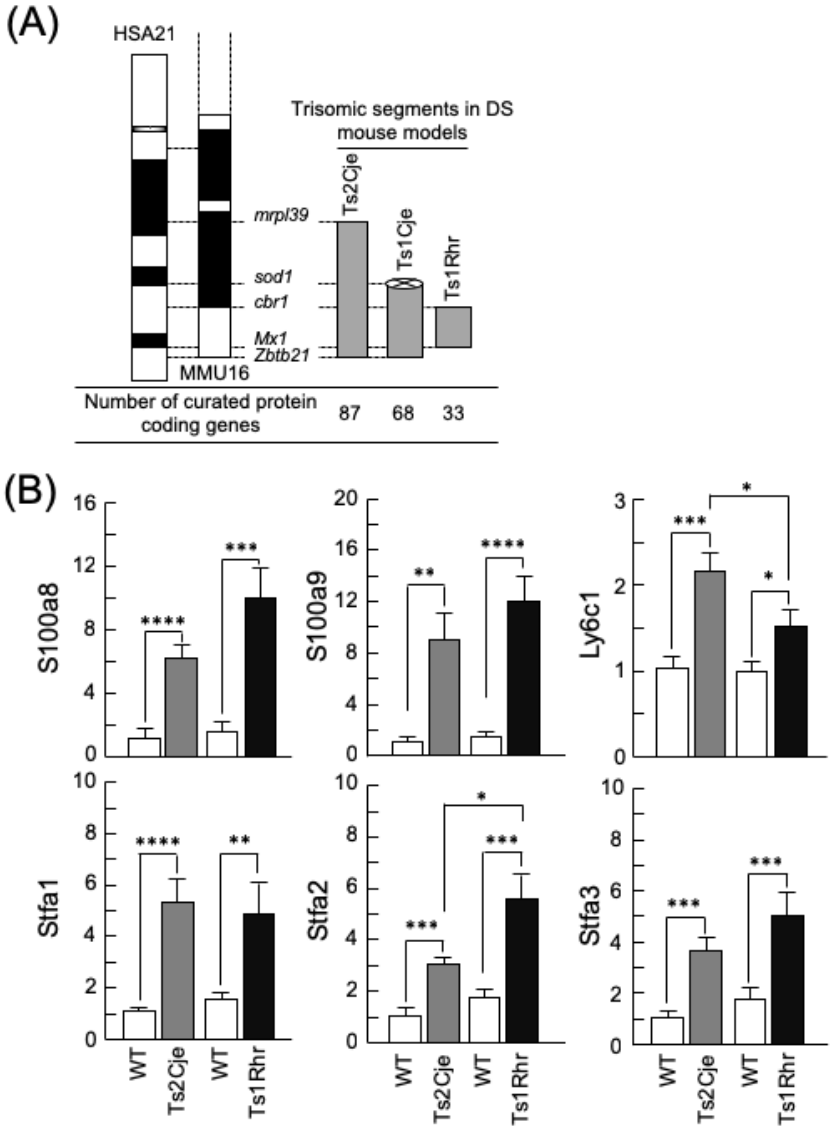

This article is protected by copyright. All rights reserved.

Accepted Article

Fig. 4 Ishihara et al.

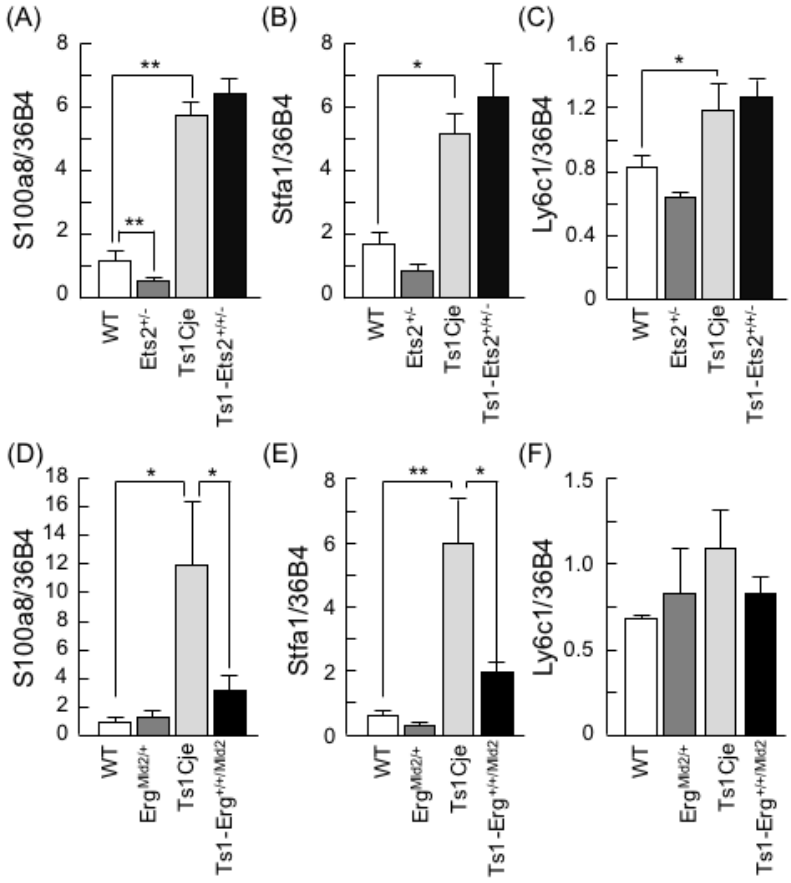

This article is protected by copyright. All rights reserved.

Accepted Article

Ishihara_Fig. 5

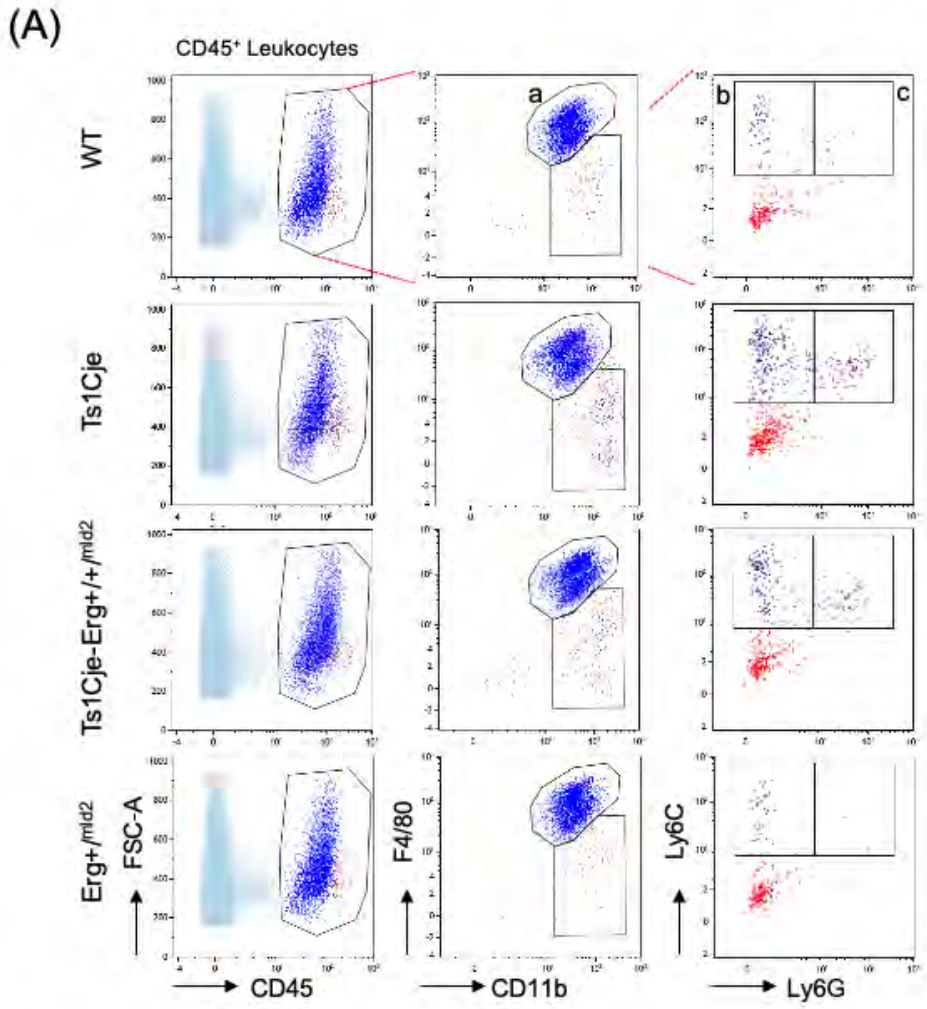

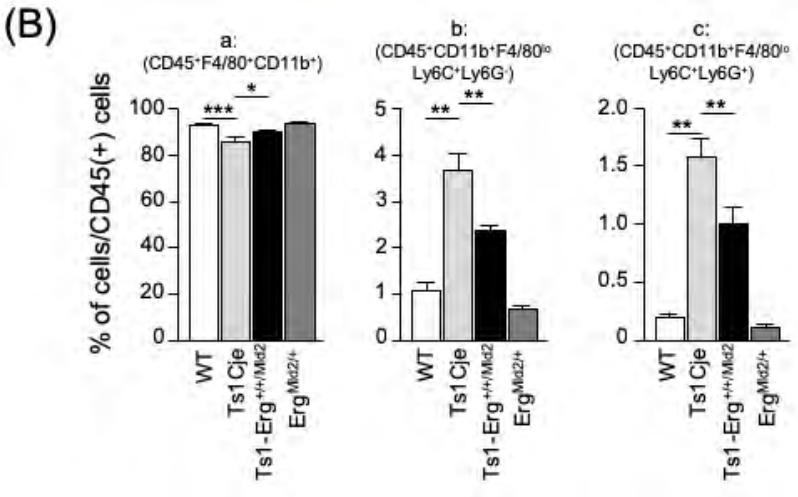

This article is protected by copyright. All rights reserved.

Accepted Article

Fig. 6 Ishihara et al.

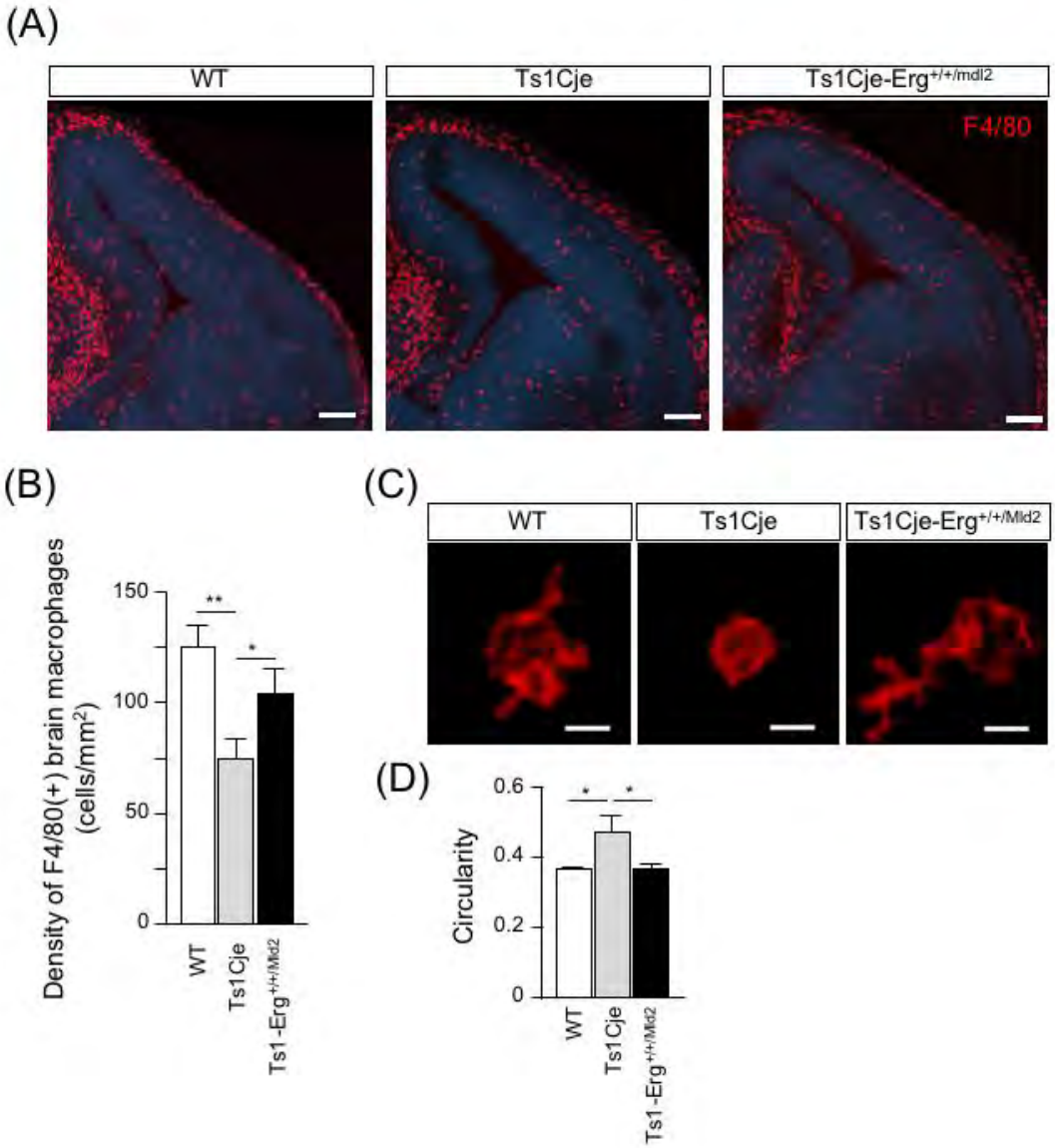

This article is protected by copyright. All rights reserved.

Accepted Article

Ishihara_Fig. 7

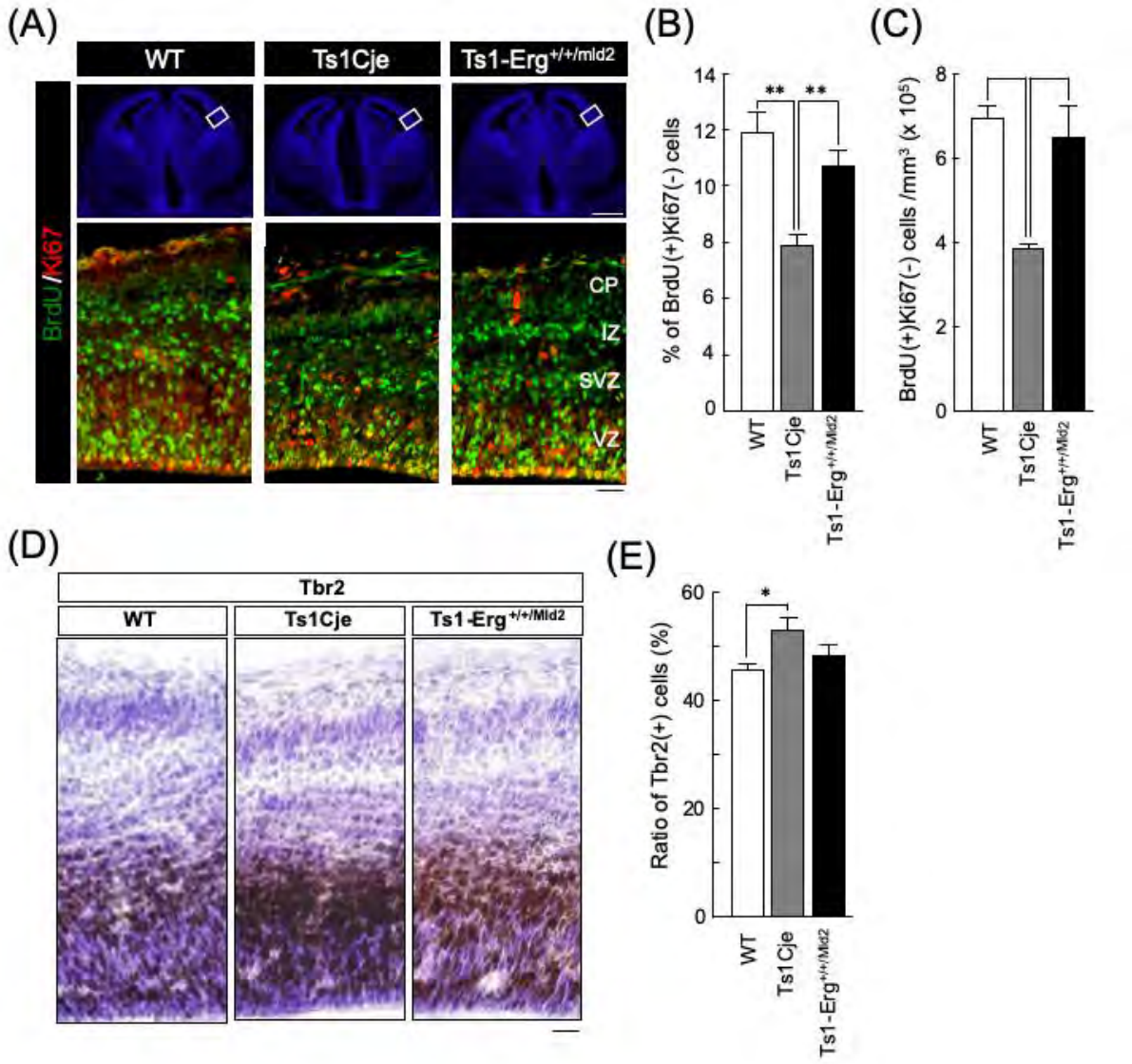

This article is protected by copyright. All rights reserved.